

Measurement range enlargement in Brillouin optical correlation-domain reflectometry based on temporal gating scheme

Yosuke Mizuno, Zuyuan He, and Kazuo Hotate

Department of Electrical Engineering and Information Systems, The University of Tokyo,
7-3-1 Hongo, Bunkyo-ku, Tokyo 113-8656, Japan
ymizuno@sagnac.t.u-tokyo.ac.jp; ka@sagnac.t.u-tokyo.ac.jp; hotate@sagnac.t.u-tokyo.ac.jp

Abstract: We newly develop a temporal gating scheme to enlarge the measurement range of Brillouin optical correlation-domain reflectometry (BOCDR) for a fiber-optic distributed strain measurement. In this scheme, the trade-off problem between the measurement range and the spatial resolution can be dissolved. 66-cm spatial resolution and 1-km measurement range were simultaneously obtained with 50-Hz sampling rate.

©2009 Optical Society of America

OCIS codes: (060.2370) Fiber optics sensors; (280.4788) Optical sensing and sensors; (290.5830) Scattering, Brillouin.

References and links

1. T. Horiguchi, T. Kurashima, and M. Tateda, "A technique to measure distributed strain in optical fibers," *IEEE Photon. Technol. Lett.* **2**, 352-354 (1990).
2. M. Nikles, L. Thevenaz, and P. Robert, "Simple distributed fiber sensor based on Brillouin gain spectrum analysis," *Opt. Lett.* **21**, 758-760 (1996).
3. T. Horiguchi, and M. Tateda, "BOTDA-nondestructive measurement of single-mode optical fiber attenuation characteristics using Brillouin interaction: theory," *IEEE J. Lightwave Technol.* **7**, 1170-1176 (1989).
4. A. W. Brown, B. G. Colpitts, and K. Brown, "Distributed sensor based on dark-pulse Brillouin scattering," *IEEE Photon. Technol. Lett.* **17**, 1501-1503 (2005).
5. Y. Koyamada, "Proposal and simulation of double-pulse Brillouin optical time-domain analysis for measuring distributed strain and temperature with cm spatial resolution in km-long fiber," *IEICE Trans. Commun.* **E90-B**, 1810-1815 (2007).
6. K. Hotate, and T. Hasegawa, "Measurement of Brillouin gain spectrum distribution along an optical fiber using a correlation-based technique – proposal, experiment and simulation," *IEICE Trans. Electron.* **E83-C**, 405-412 (2000).
7. K. Hotate, and M. Tanaka, "Distributed fiber Brillouin strain sensing with 1-cm spatial resolution by correlation-based continuous-wave technique," *IEEE Photon. Technol. Lett.* **14**, 197-199 (2002).
8. K. Y. Song, Z. He, and K. Hotate, "Distributed strain measurement with millimeter-order spatial resolution based on Brillouin optical correlation domain analysis," *Opt. Lett.* **31**, 2526-2528 (2006).
9. Y. Mizuno, W. Zou, Z. He, and K. Hotate, "Proposal of Brillouin optical correlation-domain reflectometry (BOCDR)," *Opt. Express* **16**, 12148-12153 (2008).
10. Y. Mizuno, Z. He, and K. Hotate, "One-end-access high-speed distributed strain measurement with 13-mm spatial resolution based on Brillouin optical correlation-domain reflectometry," *IEEE Photon. Technol. Lett.* **21**, 474-476 (2009).
11. T. Kurashima, T. Horiguchi, H. Izumita, S. Furukawa, and Y. Koyamada, "Brillouin optical-fiber time domain reflectometry," *IEICE Trans. Commun.* **E76-B**, 382-390 (1993).
12. A. Fellay, L. Thevenaz, M. Facchini, M. Nikles, and P. Robert, "Distributed sensing using stimulated Brillouin scattering: towards ultimate resolution," *Proc. 12th Intern. Conf. Optical Fiber Sensors*, 324-327 (1997).
13. Y. Koyamada, Y. Sakairi, N. Takeuchi, and S. Adachi, "Novel technique to improve spatial resolution in Brillouin optical time-domain reflectometry," *IEEE Photon. Technol. Lett.* **19**, 1910-1912 (2007).
14. G. P. Agrawal, *Nonlinear Fiber Optics* (Academic Press, California, 1995).
15. K. Hotate and Z. He, "Synthesis of optical-coherence function and its applications in distributed and multiplexed optical sensing," *IEEE J. Lightwave Technol.* **24**, 2541-2557 (2006).
16. M. Kannou, S. Adachi, and K. Hotate, "Temporal gating scheme for enlargement of measurement range of Brillouin optical correlation domain analysis for optical fiber distributed strain measurement," *Proc. 16th Intern. Conf. Optical Fiber Sensors*, 454-457 (2003).

1. Introduction

Many fiber-optic strain/temperature sensors have been proposed based on various phenomena including scattering, optical loss, and polarization. In particular, much research interest has been focused on sensors utilizing Brillouin scattering, in which the Brillouin frequency depends on the longitudinal strain and the temperature change in the optical fiber, thus allowing the distributed measurement of strain and/or temperature along the fiber [1]-[11].

Brillouin scattering-based distributed fiber-optic sensors are classified into two types: "reflectometries", in which a light beam is injected into one end of the fiber under test (FUT), and "analysis systems", in which two light beams are injected into both ends of the FUT. Several kinds of analysis systems have been studied, including the Brillouin optical time-domain analysis (BOTDA) [3]-[5] and the Brillouin optical correlation-domain analysis (BOCDA) [6]-[8]. Although those systems utilizing the stimulated Brillouin scattering (SBS) can obtain relatively large signals, they need two-end access, which is often not feasible in a long-range measurement, and cannot work completely when the FUT has even one breakage point. Thus, for some practical applications, one-end access reflectometries are more favorable, even though their signal is not as large because they utilize the spontaneous Brillouin scattering.

Recently, we have proposed Brillouin optical correlation-domain reflectometry (BOCDR) [9]-[10] to measure the strain distribution along an FUT from a single end of the fiber. In a pulse-based conventional Brillouin optical time-domain reflectometry (BOTDR) [11], the spatial resolution is generally limited by a combination of linewidth broadening and signal weakening associated with the use of short optical pulses. The best spatial resolution for basic systems is typically 1 m [12], though some progress has been made to enhance the resolution further [13]. On the contrary, by controlling the interference of continuous lightwaves, BOCDR shows such unique features as random access to measuring positions, high spatial resolution, and high sampling rate. In our previous experiments, 13-mm spatial resolution has been obtained with 50-Hz sampling rate, while the total measurement time depends on the number of sensing points over the FUT [10].

However, BOCDR suffers from a trade-off between the measurement range and the spatial resolution. Their ratio N_R was fixed at approximately 580 due to the limitation of Rayleigh scattering [9]. This means that, for example, when the spatial resolution was 40 cm or 13 mm, the measurement range was 224 m [9] or 7.6 m [10], respectively. Thus, in order to achieve kilometer-order measurement range, the spatial resolution must be about 2 m or larger, which is even worse than that of BOTDR.

In this paper, we newly implement a temporal gating scheme to obtain higher N_R , namely, to enlarge the measurement range of BOCDR while maintaining the spatial resolution. In this scheme, any correlation peak within the FUT can be arbitrarily selected, so that multiple correlation peaks can be utilized. 66-cm spatial resolution and 1-km measurement range ($N_R = 1515$) were simultaneously achieved with 50-Hz sampling rate.

2. Principle

When a light beam is injected into an optical fiber, backscattered light (Stokes light) is generated through the interaction with acoustic phonons. This phenomenon is called spontaneous Brillouin scattering. The Brillouin-scattered light spectrum, also known as the Brillouin gain spectrum (BGS), takes the shape of Lorentzian function [14]. The frequency at which the peak power is obtained in the BGS is shifted for about 11 GHz from the incident light frequency when the incident light wavelength is 1.55 μm . This amount of frequency shift is called the Brillouin frequency shift (BFS) f_B . If tensile strain or temperature change occurs in the fiber, the BFS varies in proportion to the applied strain (1 MHz / 0.002 %) or

temperature change (1 MHz / 1 K). Therefore, by measuring the distribution of the BFS along the FUT, the applied strain amplitude or temperature change can be derived.

In the basic BOCDR, the Stokes light due to the spontaneous Brillouin scattering of the pump light in the FUT is heterodyned with the reference light (self-heterodyne scheme) [9]. In order to resolve the strain-applied position, the pump light and the reference light are sinusoidally frequency-modulated, producing periodical correlation peaks along the FUT [15]. The measurement range of conventional BOCDR, that is, the interval of the correlation peaks d_m is given by:

$$d_m = \frac{V_g}{2f_m}, \quad (1)$$

where V_g is the group velocity of light and f_m the modulation frequency. If we utilize a non-0th correlation peak (where the 0th peak is defined at the zero optical path-difference position), the position of the correlation peak can be moved along the FUT by changing f_m . Hence, distributed strain measurement can be performed by controlling f_m . The spatial resolution Δz is given by:

$$\Delta z = \frac{V_g \Delta\nu_B}{2\pi f_m \Delta f}, \quad (2)$$

where $\Delta\nu_B$ is the Brillouin gain bandwidth (~ 30 MHz) in optical fibers, and Δf the modulation amplitude of the light source [6]. The number of effective sensing points N_R , which can be regarded as the evaluation parameter, is given by the ratio between d_m and Δz , as:

$$N_R = \frac{d_m}{\Delta z} = \frac{\pi \Delta f}{\Delta\nu_B}. \quad (3)$$

From Eq. (3), in order to enhance the measurement range substantially, Δf needs to be increased. However, it is difficult to increase Δf higher than a half of the BFS of the fiber (about 5.4 GHz for standard SMFs) [9]. Another way to enhance the measurement range is to utilize multiple intervals of the correlation peaks. In this case, we select only one correlation peak for distributed measurement, but suppress other peaks to avoid cross-talk. Therefore, the measurement range is multiplied. The temporal gating scheme is an effective method for this purpose, and has been applied to BOCDA [16, 17].

The concept of the temporal gating scheme in BOCDR is explained, referring to an experimental setup depicted in Fig. 1(a). The pump light is converted into optical pulses by an intensity modulator (IM), as shown in Fig. 1(b). By setting the pulse width, t_w , to be the same as the interval of correlation peaks:

$$t_w = \frac{1}{2f_m}, \quad (4)$$

the Stokes light from each correlation peak can be temporally resolved. The interval of optical pulses is set to double the length of the FUT to avoid the overlap of reflected signals. In addition, by adjusting the relative phase, at the right time when the Stokes light from a particular correlation peak returns, it is heterodyned with the reference light, which is also converted into optical pulses with the same width t_w . Thus, it becomes possible to arbitrarily select any particular correlation peak within the FUT.

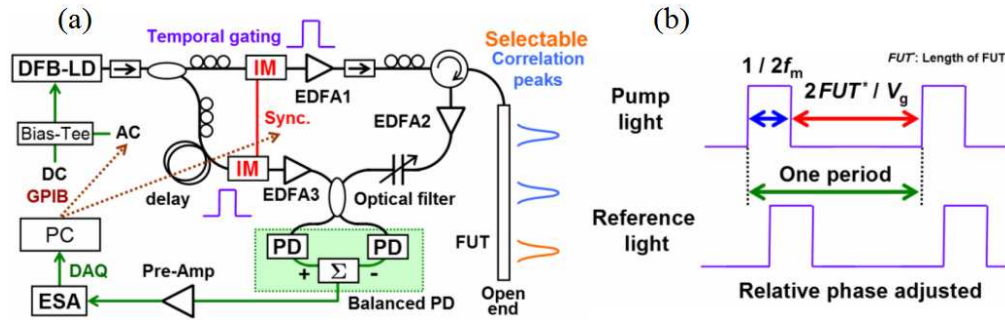


Fig. 1. (a). Experimental setup of the BOCDR with a temporal gating scheme. (b) Pulse shapes of the pump light and the reference light.

3. Experiments

The experimental setup is depicted in Fig. 1(a). A distributed-feedback laser diode (DFB-LD) at frequency $f_0 = 193.15$ THz (1552 nm) was used as a light source, and a sinusoidal frequency modulation was applied to generate correlation peaks within an FUT. The output from the LD was divided into two light beams by a coupler. One of the beams was directly used as the reference light of self-heterodyne detection, after passing a 5-km delay fiber for controlling the order of periodical correlation peaks and an Er-doped fiber amplifier (EDFA) for enhancing the heterodyned beat signal. The other beam was injected into the FUT as the pump light, after being amplified by a high-power EDFA to 28 dBm. The weak Stokes light at frequency $f_0 - f_B$, backscattered from the FUT, was amplified again by an EDFA. An optical filter composed of fiber Bragg grating (FBG) with a 3-dB bandwidth of about 10 GHz was inserted after the EDFA in order to suppress the Rayleigh scattering and the Fresnel reflection in the FUT at frequency f_0 . The optical beat signal of the reference light and the Stokes light was detected by balanced photo-diodes (PDs) and converted to an electrical signal. The relative polarization state of the two light beams was optimized by adjusting polarization controllers manually. After 15-dB amplification from an electrical pre-amplifier, the signal was monitored by an electrical spectrum analyzer (ESA). The measurement data were transferred to a personal computer (PC). Two LiNbO₃ IMs were set in the pump and reference paths for the temporal gating scheme.

The structure of the FUT is shown in Fig. 2. It was composed of a 1-km standard single-mode fiber (SMF), in which about 0.1-% strain was applied to a 3-m section (990 - 993 m) fixed on a translation stage using epoxy glue (It is difficult to apply accurately 0.1-% strain to a section as long as 3 m due to the FUT's own weight). One end of the FUT was spliced to a circulator, and the other end was kept open. The overall sampling rate of the measurement for a single position was 50 Hz.

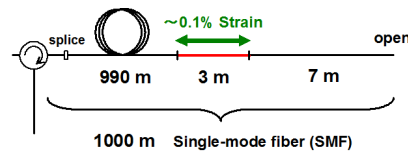


Fig. 2. Structure of the FUT.

In order to experimentally confirm that, without the temporal gating scheme, the measurement cannot be performed correctly if there are multiple correlation peaks within the FUT, first, we consider the case where there is no undesired correlation peak ($N = 0$). The modulation frequency f_m was 68.40 – 68.84 kHz, which corresponds to a measurement range

d_m of 1.5 km according to Eq. (2). The amplitude of the frequency modulation Δf was 5.4 GHz, and the nominal spatial resolution Δz was calculated to be about 2.6 m from Eq. (1).

Figure 3(a) shows the measurement result of the distribution of the BGS along the FUT. The BGS at the strain-applied section is recognized. Figure 3(b) shows the distribution of the BFS. We can see that 3-m strain was successfully detected. The change of the BFS was about 60 MHz, which agrees with the applied strain of about 0.1 %. The accuracy of the measurement at a single position was about ± 5 MHz, which corresponds to the strain of ± 0.01 % ($\pm 100 \mu\epsilon$) in this experiment.

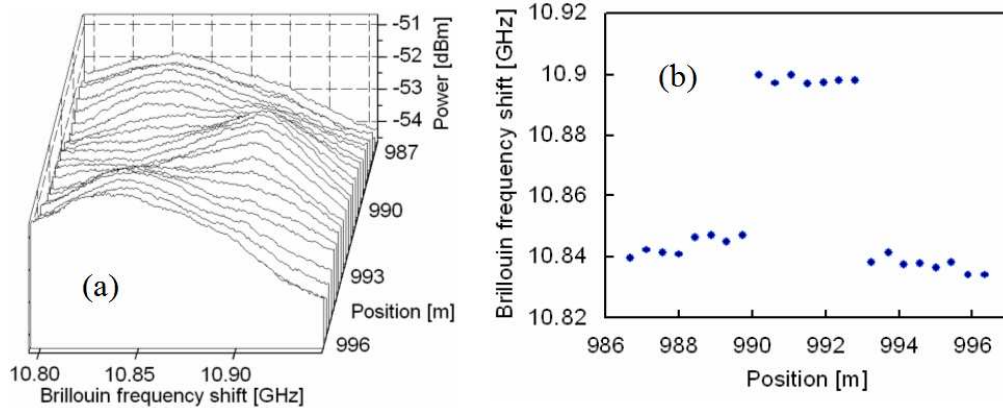


Fig. 3. Distribution of (a) BGS, and (b) BFS.

Next, we consider the effect of multiple correlation peaks within the FUT. By adjusting the modulation frequency f_m and the amplitude of the frequency modulation Δf , the spatial resolution was constantly kept to 2.6 m, with one of the correlation peaks within the strain-applied section. The interval between the correlation peaks was set to 1.5 km, 753 m, 377 m, 188 m, and 94 m, which correspond to the cases where there are 0, 1, 2, 4, and 9 undesired correlation peaks in the 1-km FUT, respectively.

As shown in Fig. 4, when there is no undesired correlation peak ($N = 0$), the BGS has its peak at about 10.9 GHz corresponding to the applied strain. However, when there is one undesired correlation peak ($N = 1$), the peak at 10.9 GHz is overlapped with that at 10.85 GHz corresponding to zero strain, which makes distributed strain measurement impossible. The further the number of the undesired peaks is increased, the larger the peak at 10.85 GHz becomes, and so the peak at 10.9 GHz becomes unobservable. Thus, it was confirmed that the basic BOCDR measurement without the temporal gating scheme cannot be performed correctly if there are multiple correlation peaks within the FUT.

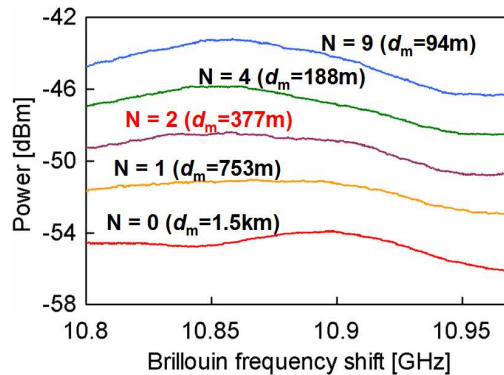


Fig. 4. Measured BGS without the temporal gating scheme applied, when there are multiple correlation peaks within the FUT. The length of the FUT is 1 km. d_m represents the interval between the correlation peaks, and N the number of undesired peaks within the FUT.

Then, we confirmed the operation of the temporal gating scheme, using the two LiNbO₃ IMs inserted before the EDFAs in the pump and reference paths in Fig. 1(a). The same 1-km SMF was used as the FUT, in which strain was applied to the same 3-m section (990 - 993 m). The modulation frequency f_m was 276.1 kHz, which corresponds to a 377-m interval of correlation peaks according to Eq. (1). This means that there are three correlation peaks (two undesired peaks) within the FUT. The amplitude of the frequency modulation Δf was set to 1.4 GHz, and the spatial resolution Δz was calculated to be 2.6 m from Eq. (2). These conditions are almost the same as those for the experiment already described above (See Fig. 4, $N = 2$). According to Eq. (4), the width and the period of the optical pulses were set to 1.81 μ s and 11.50 μ s, respectively (duty cycle = 15.7 %). The overall sampling rate of the BGS measurement for a single position was 50 Hz.

The changes of the BGS with and without strain applied when each peak was selected are shown in Figs. 5(a)-5(c). The relative phase differences of optical pulses were 226, 113, and 0 degrees for Figs. 5(a), 5(b), and 5(c), respectively, where a positive phase difference means that the phase of the reference pulses is faster than that of the pump pulses. In Figs. 5(a) and 5(b), the BGS shows hardly any change because the selected correlation peaks are outside the strain-applied section. On the contrary, in Fig. 5(c), the peak of the BGS shifts because the selected correlation peak is within the strain-applied section. Thus, the temporal gating scheme was confirmed to be effective.

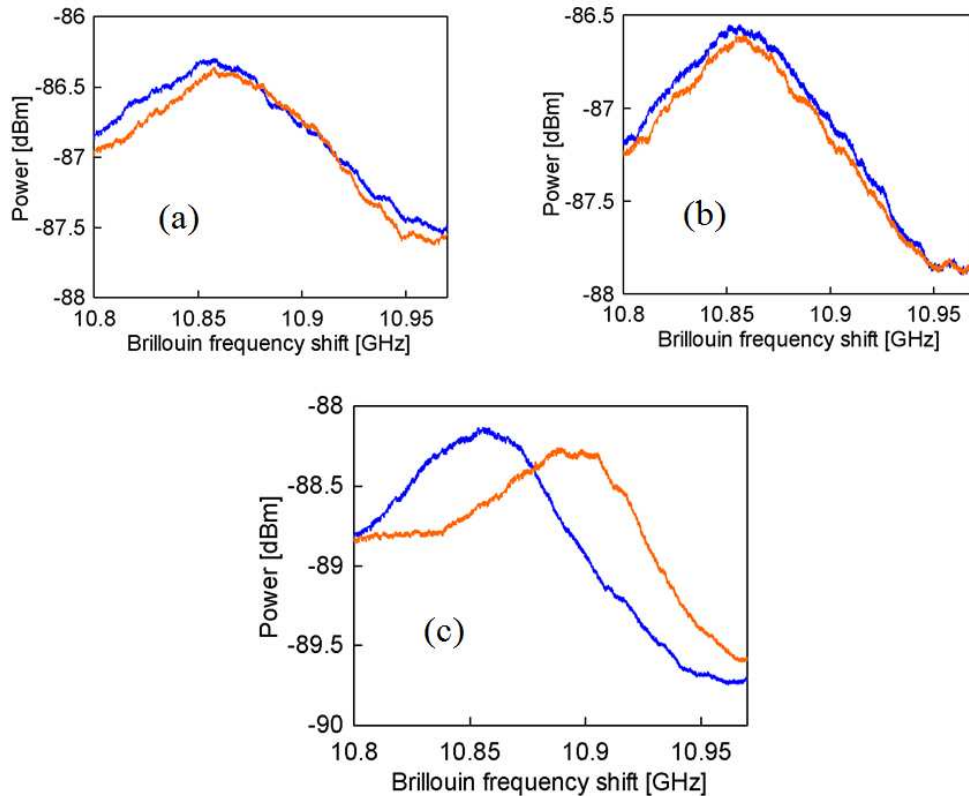


Fig. 5. Measured BGS when (a) the first, (b) the second, and (c) the third correlation peaks were selected, with (blue) and without (orange) strain applied to the section corresponding to the third correlation peak.

Finally, a distributed strain sensing based on the temporal gating scheme was performed. Figure 6 shows the structure of the FUT. 0.3-% strain was applied to a 90-cm section (990 –

990.9 m). The modulation frequency f_m was 275.65 – 276.25 kHz, and the amplitude of the frequency modulation Δf was set to 5.4 GHz, and so the spatial resolution Δz was calculated to be 66 cm. Figures 7(a) and 7(b) show the measurement results of the distribution of the BGS and the BFS, respectively. The strain-applied 90-cm section was clearly detected. The change of the BFS was about 150 MHz, which is in good agreement with the applied strain of 0.3 %. The accuracy of the measurement at a single position was about ± 20 MHz, which corresponds to a strain resolution of ± 0.04 % ($\pm 400 \mu\epsilon$) in this experiment.

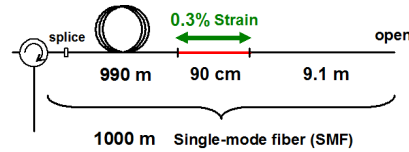


Fig. 6. Structure of the FUT.

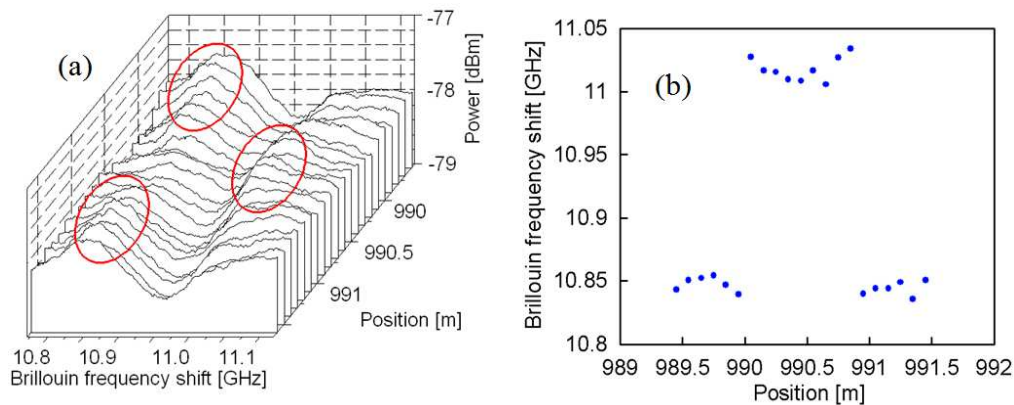


Fig. 7. Distribution of (a) BGS, and (b) BFS.

Thus, we succeeded in achieving 1-km measurement range and 66-cm spatial resolution simultaneously. Their ratio N_R is calculated to be 1515, which is about three times as large as that of the basic BOCDR system (about 580). In order to enhance N_R further, the S/N ratio of the system must be improved. We think further research is needed on this point.

4. Conclusion

In this paper, a temporal gating scheme was newly developed to enlarge the measurement range of the BOCDR system while maintaining the high spatial resolution. 66-cm spatial resolution and 1-km measurement range were simultaneously achieved with 50-Hz sampling rate. This means that the ratio between the measurement range and the spatial resolution was enhanced from the conventional value 580 to 1515. We expect that the BOCDR system will become a promising technology for practical use as a fiber-optic nerve system in the smart materials and structures.

Acknowledgments

The authors are grateful to Dr. Weiwen Zou at the University of Tokyo, Japan, for helpful discussions and comments. Yosuke Mizuno thanks the Japan Society for the Promotion of Science (JSPS) Research Fellowships for Young Scientists. This work was supported by the “Grant-in Aid for Creative Scientific Research” and the “Global Center of Excellence (G-COE) Program” from the Ministry of Education, Culture, Sports, Science and Technology (MEXT), Japan.